

A clustered speckle approach to optical trapping

J.P. Staforelli^a, J.M. Brito^a, E. Vera^a, P. Solano^a, A. Lencina^{b,*}

^a Center for Optics and Photonics, Universidad de Concepción, Casilla 160-C, Concepción, Chile

^b Centro de Investigaciones Ópticas (CONICET La Plata - CIC), C.C. 3, 1897 Gonnet, Argentina

An *in situ* study of the clustered speckle 3D structure using an optical tweezer setup is presented. Clustered speckles appear when a coherently illuminated diffuser is imaged through a pupil mask with several apertures, properly distributed over a closed path, which is placed before the objective lens of a standard optical trapping system. Thus, light volumes are reduced several times when compared with standard speckles, being even smaller than the focus volume of a Gaussian beam commonly used to trap. Moreover, clustered speckles have odd statistical properties which differentiated it from standard speckles. Then, geometrically ordered multiple trapping arrays, with statistical random distribution of intensities, can be created with this technique. This fact could enable different studies concerning optical binding or new developments in coherent matter wave transport where Optical Trapping has been proven with standard speckles. In this work, a qualitative analysis of clustered speckles in an optical tweezer setup relative to the number of apertures in the mask and their size is carried on. Besides, in the Rayleigh regime, a general quantitative method to characterize the trapping capability of an optical field is proposed. Then, it is applied to clustered speckles. As a result, a relation between aperture size and the maximum size of the particles that could be trapped is found. This fact opens the possibility of engineering the statistic of the trapped particles by properly selecting the pupil mask.

1. Introduction

Nowadays, Optical Trapping (OT) and manipulation of particles by laser beams are well-established techniques for manipulating micro- and nano-sized particles and molecules [1,2]. Since its introduction, OT has evolved in several ways: laser wavelengths have been moved to infrared to avoid damage in biological tissue [3]; trapping forces are now accurately measured [4]; field calculations are readily performed with recent theoretical developments [5]; holographic diffractive elements are used for creating multi-trap setups [6], etc. These improvements have led to surprising experiments and results [7], widely discussed in the literature. Nonetheless, randomized intensity distributions, such as speckle fields, have rarely been studied and used in trapping arrangements.

Although speckle fields seem suitable for trapping nanometer objects, only just a decade ago they were proposed to trap (and cool) atoms [8,9]. In trapping experiments, an accurate mapping between the intensity of the speckle field and the atomic density was found. Moreover, different longitudinal and transversal temperatures were measured and related with the characteristic length of the speckle field in cooling setups. Those contributions, combined with the improvement in handling cold atoms, have led to developments concerning atoms in

random potentials, mainly oriented to atomic properties, but without a thorough revision of the spatial statistical properties of the speckle field [10,11]. Therefore, reviewing the 3D structure of the speckle field seems to become a required task. More recently, photophoretic forces for trapping has been induced in carbon agglomerated nanoparticles using standard speckle fields [12]. Highly stable confinement and size selection are shown. The smallest particles remain-trapped in the dark regions of the speckle pattern, this kind of traps are called *bottle beam traps*. That paper reviews a qualitative description of the 3D standard speckle distribution and gives new possibilities to confine particles instead of the commonly used bright regions.

Generally, intensity limitations that appear due to the usual low efficiency in obtaining a speckle field impose a limit to the trapping force for more massive objects than atoms like quantum dots, molecules, and a wide range of micron and nano-sized particles. However, current holographic techniques can lead to high intensity pseudo-random speckle-like fields by using LCD based SLM, overcoming the intensity restriction. Another drawback to use speckle fields for trapping is related to the Rayleigh limits to visualize nanometric particles. Nevertheless, recent developments in microscopy imaging succeed in resolve below 100 nm at nearly video frame rates [13]. This fact encourages the use of speckle fields in optical traps with emphasis, more particularly, in geometrically ordered speckle field distributions, which are candidates to conform regular arrangements of traps. The arrangement that we propose is called clustered speckle pattern, and is the main point to be discussed in this paper.

As it is well-known, speckle fields appear when a laser is reflected from (or pass through) a rough surface. In this case, cigar-shaped light volumes appear and it is well-established that speckle size depends on the illuminated area. Similar results appear when the speckle field is imaged by a lens, but now its size depends on the lens pupil-mask diameter. Both results come from the field intensity correlation assuming only one circular (or square) illuminated area. However, when the illuminated area is not simply connected, speckle size and shape changes. In particular, for ring-slit aperture pupil masks, speckle fields acquire a string or network-like appearance. In fact, Clustered Speckles (CS) were introduced by attaching a ring-slit aperture pupil mask to a diffuser [14]. Lately, Lencina et al. [15] have studied the cluster formation in imaging systems by representing a ring-slit aperture as a limiting case of a discrete arrangement of apertures uniformly distributed on a circumference. Then, the cluster formation is interpreted as intra speckle modulations generated by the multiple interference patterns produced by the apertures in the pupil. Note that, each pair of apertures generates an interference pattern that modulates each individual speckle. By increasing the number of apertures, the number of interference patterns increases, each one with its corresponding direction and spatial frequency. Coherent addition of these patterns produce those light spots be arranged in preferred positions, originating then, the CS. Broadly speaking, CS appear when a diffuser is imaged through a lens with an attached pupil mask having several apertures properly distributed over closed paths. For a proper combination of pupil parameters, the cluster spots are found on regular arrangements where a symmetrical version of the aperture distribution in the pupil is reproduced [16]. These particular CS are so called 'regular cluster'. The CS strongly modify the 3D intensity distribution of the field, and therefore the spatial intensity correlations, compared to standard speckles. This fact makes that a proper model for CS anywhere after the lens and for their 3D correlations be still a subject of research. Regardless, it is observed that in CS, light volumes are reduced several times when compared with standard speckles, being even smaller than the focus volume of a Gaussian beam (necessary to trap with a single optical tweezers). Thus, geometrically ordered multiple trap arrays with statistical random distribution of intensities may be created with this technique. These multiple traps will have different statistical distributions according to the distribution of the apertures in the pupil and its sizes. This peculiarity will enable different studies concerning, e.g., optical binding and coherent matter wave transport with random potentials having different statistical properties. Additionally, this paper suggests new extensions of current applications of bottle-beam traps for sub-micron sized particles in speckle fields.

All the hereinbefore mentioned arguments have encouraged us to carry out an *in situ* study of the CS as a first approach to be considered in OT. Then, a qualitative analysis concerning the number of apertures in the pupil mask and their size is carried on. Finally, pointing out to particles in the Rayleigh regime, a general method which allows to put an upper bound to the particle size that an optical field might trap is developed. This method is therefore applied to find the size of the particles that the CS could trap.

The work is organized as follows: in Section 2 the experimental setup and technical details are sketched out; Section 3 is organized in subsections where the transversal and longitudinal intensity profiles are qualitatively analyzed (Subsection 3.1 and 3.2), and the method for characterizing the trapping capability of an optical field and its application to CS is developed (Subsection 3.3); and finally in Section 4, the conclusions are established.

2. Experimental setup

The setup employed is depicted in Fig. 1. An expanded doubled-Nd:YAG laser beam strikes a diffuser and becomes a speckle field. It passes across a pupil mask and is focused by an Edmund Optics 40x DIN microscope objective. The field in the neighborhood of the objective focus is

imaged by a 60x DIN microscope objective, also from Edmund Optics, and recorded in a monochrome CMOS uEye camera (1.3 Mpixel). A set of 1 μm , 2 μm , 3 μm and 4 μm calibrated particles from Kisker-Biotech is used for spatial calibration. For each particle size, its diameter is measured when focused on the camera. Then, from a linear regression applied to a particle size versus pixel plot, the calibration results 0.135 $\mu\text{m}/\text{pixel}$.

Imagery data is collected for pupil masks having one, six or ten circular apertures whose diameters are 465 μm or 900 μm . For the pupil with one aperture, it is centered on the optical axis of the system. In the other cases, apertures are evenly distributed on a circumference of 4 mm diameter (see right-inset in Fig. 1). To define the region where images should be taken, the diffuser and the pupil are previously removed and the focus of the system is found (see left-inset in Fig. 1). Afterwards, successive images are taken along the optical axis (z-direction) ranging from $-50 \mu\text{m}$ to $+50 \mu\text{m}$ measured from the focus, with steps of 1 μm . Small step-to-step lateral errors coming from both, the translational stage and minor misalignments, are corrected by using subpixel image registration techniques [17].

3. Results and discussions

3.1. Transversal intensity profile

Fig. 2 shows the in-focus speckle field transversal intensity in an OT. The results of the first, second and third column correspond to the one, six and ten apertures cases, respectively; whereas rows are for 465 μm and 900 μm aperture diameter. Note that the figure scale for the single aperture case is twice the others. As expected, the speckle field tends to cluster when multiple apertures are used. This cluster reduces the speckles transversal dimensions to small spots ($<1 \mu\text{m}$ diameter) when compared to the one aperture case. Multiple apertures, which introduce intensity modulations whose spatial frequency is inversely proportional to their separation, originate the cluster formation. For apertures distributed on a circumference, those pairs which are diametrically opposed dominate the modulation and therefore clusters tend to have an annular shape. On the other hand, the aperture size determines the regularity of the cluster, i.e. for smaller apertures the cluster tends to be a regular cluster. It can be understood in this way: by thinking the cluster as intensity modulations inside a speckle, as far as the aperture size diminishes, the speckle diameter grows and more modulations can take place inside them. Then, it reduces the possibility that the cluster be perturbed by other decorrelated speckles. This behavior is a general feature of the aperture size effect on transversal intensity profiles. How annular-like is the cluster depends on a combination of aperture separations and number. An illustrative explanation is as follows: the diameter of cluster spots and the circumference diameter where they are arranged are determined by the circumference diameter where apertures are distributed. This determines how many spots can form the cluster, then how many apertures are necessary to form a well-defined annular cluster. In summary, CS are obtained by introducing multiple aperture pupil masks. The lateral dimensions of these fields are less than 1 μm , which makes them suitable candidates for generating trapping-like interaction forces in submicrometric particles, further, spatially well-defined due to the geometrical order of the CS field distribution. However, in order to establish a trapping procedure, it is also necessary to know the longitudinal structure of the field.

3.2. Longitudinal intensity profile

The longitudinal speckle field behavior in the focus neighborhood is shown in Fig. 3. Rows and columns are as in Fig. 2, and the transversal scale for the one aperture case is also twice that of the other cases. Notice that a focusing effect is observed in all figures, because image formation occurs at $z \approx 250 \mu\text{m}$. This effect is particularly evident for one aperture. Nonetheless, note that for multiple apertures, this effect is disguised by the intensity modulation introduced by the apertures,

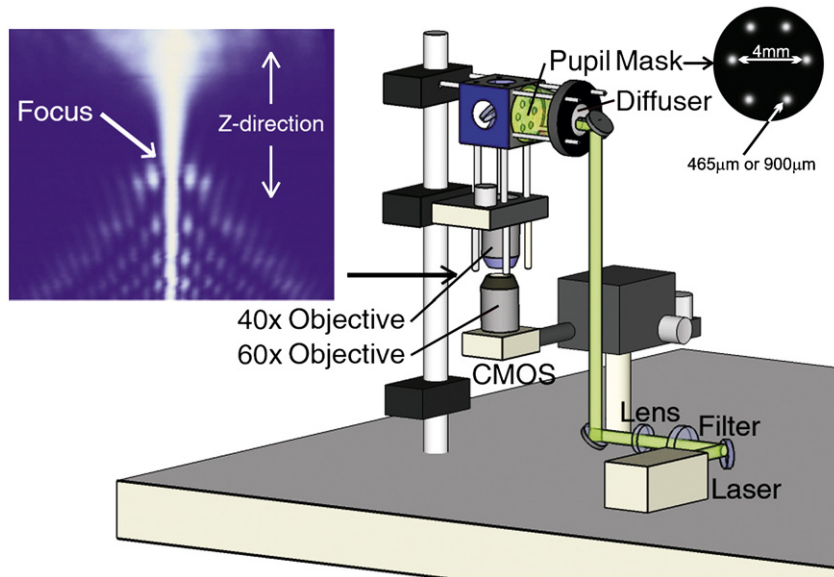


Fig. 1. A standard optical tweezer system is adapted in order to generate CS. Left-inset reveals the longitudinal section of the 3D focus along the optical axis when both, diffuser and pupil mask, are removed. Right-inset sketches the pupil mask details. It shows aperture positions and distribution for the six aperture case. In the case of only one aperture, it is centered on the pupil.

finally shortening the speckle length in the cluster. Moreover, at a first glance an increase in the aperture size does not seem to modify appreciably the cluster length. Nevertheless, there seems to have a tendency to increase the cluster length as far as diminishes the aperture size, in accordance to what it is expected in standard speckles, but limited by the longitudinal modulation that the separation of the apertures imposes. These geometrical CS features lead to consider them as suitable for trapping. However, in order to definitively prove its viability, an analysis of the intensity gradient is also required.

3.3. Gradient analysis and trapping capability

The approach presented in this paper proposes a phenomenological and general quantitative method to define the trapping capability of submicrometric particles in the Rayleigh regime considering

aperture size as a parameter. Only the bright tiny spots from the CS are chosen to discuss with this method. Otherwise, a more appropriate analysis should be considered when dealing, for instance, with void volume for trapping in a standard speckle pattern [12], but it is out of the point of this work. The case of ten apertures of 900 μm diameter is selected for intensity gradient analysis. In Figs. 2 and 3 (third column, second row), the chosen regions are indicated by dashed lines. Five order interpolation is used to allow gradient calculus with subpixel resolution. Fig. 4(a) and (b) shows the intensity gradients corresponding to Figs. 2 and 3, respectively. In Fig. 4(b), the gradient in z is augmented by a factor of ten to improve visualization. Insets for each figure show the norm of the intensity gradient. Longitudinal peak values are in the order of $0.28 \mu\text{m}^{-1}$. From Fig. 4(a), it is clear the existence of a transverse potential-well pointing to the intensity maximum. In the same way, Fig. 4(b) shows a

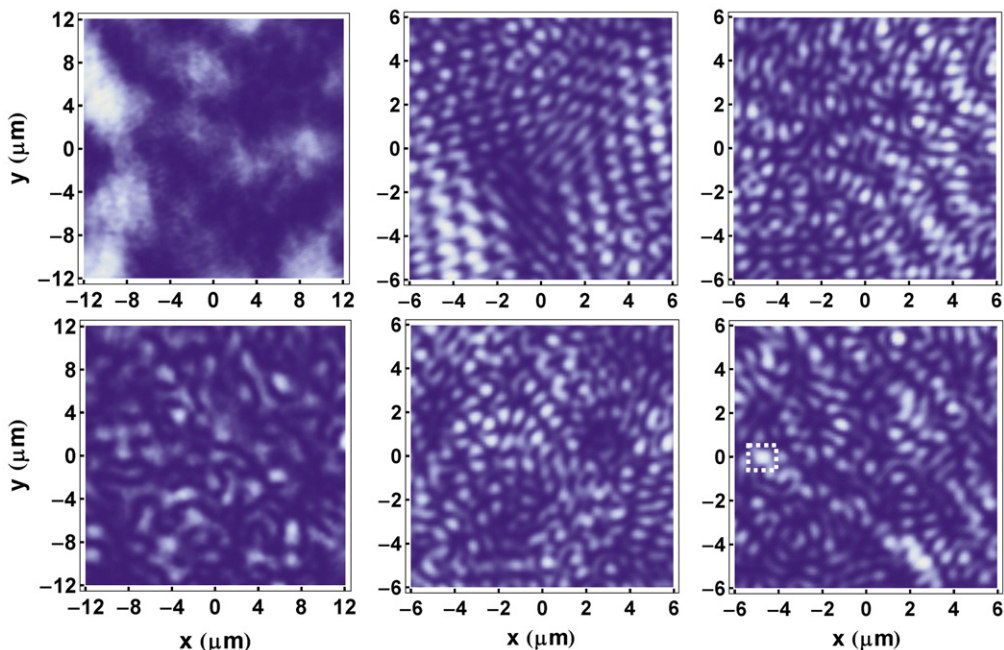


Fig. 2. Transversal in-focus speckle field intensity. Rows are for 465 μm and 900 μm aperture size. Columns are for one, six and ten apertures.

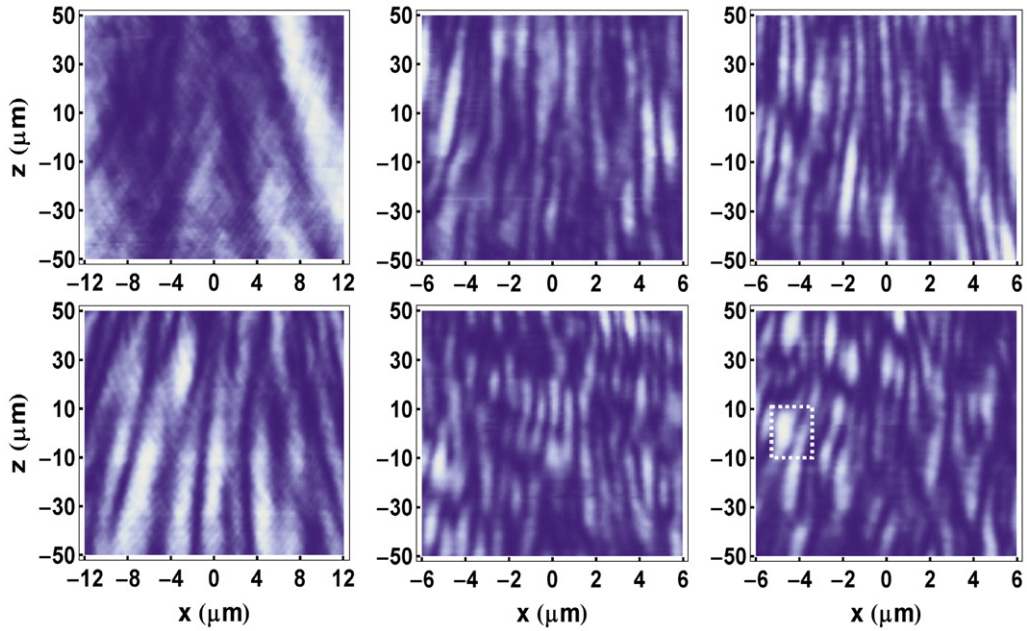


Fig. 3. Longitudinal speckle field intensity in the focus neighborhood. Rows are for 465 μm and 900 μm aperture size. Columns are for one, six and ten apertures.

shallow potential well along the longitudinal direction. Insets clearly show the existence of a volume of null gradient where a particle could be trapped. In the Rayleigh regime, an effective trapping takes place when the longitudinal *gradient* force overcomes the *scattering* one [18]. For a sphere of radius a , the quotient of these forces reads

$$\frac{F_{\text{grad}}}{F_{\text{scatt}}} = \frac{3\lambda^4}{64\pi^4 n_m a^3} \frac{(m^2 + 2)}{(m^2 - 1)} \frac{\partial(\ln I)}{\partial z} \quad (1)$$

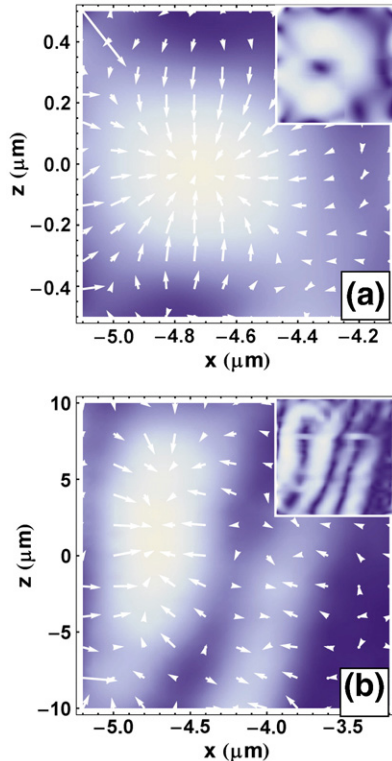


Fig. 4. Intensity gradient of the speckle field intensity, (a) transversal, from Fig. 2; (b) longitudinal, from Fig. 3. Insets, norm of the intensity gradient.

where λ is the vacuum laser wavelength, n_m is the refractive index of the surrounding medium, m is the refractive index ratio of the particle to the medium, and I is the field intensity. This equation allows the analysis of a particular situation in the following way: for a given wavelength, say 0.532 μm , take the index of refraction for both, particles and medium, for instance polystyrene and water. Then, a log-log plot of the derivative of the intensity per unit intensity versus particle radius yields to know which particles can be trapped in a particular field. Fig. 5 shows the referred plot. The region where Eq. (1) is greater than unity is clipped in red. As mentioned, the peak longitudinal gradient in Fig. 4(b) is around 0.28 μm^{-1} , and it takes place approximately when the intensity drops out to a half of its peak value. Thus, the derivative of the intensity per unit intensity reaches 0.56 μm^{-1} . This value is shown in Fig. 5 as a white line, and the intersection with the curve where Eq. (1) equals the unity is indicated with a dashed line. This result allows to anticipate that these CS may

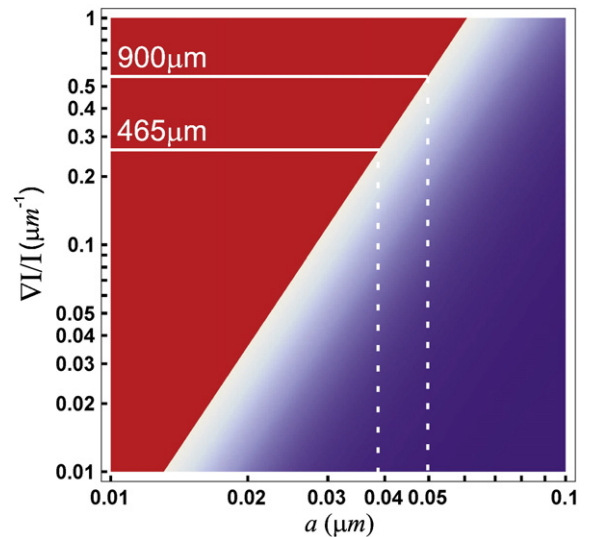


Fig. 5. $F_{\text{grad}}/F_{\text{scatt}}$ as function of $\nabla I/I$ and particle size. $F_{\text{grad}}/F_{\text{scatt}} > 1$ (top-left region) was clipped in red.

trap Rayleigh particles smaller than 50 nm for the employed wavelength. The result for apertures of 465 μm is also displayed in Fig. 5. It is apparent that there is a relationship between the particle size that can be trapped and the aperture size. For smaller apertures, the light volume increases longitudinally. This fact implies that intensity gradients be lower in modulus. Then, if it is assumed that the maximum gradient takes place when the intensity decreases by a half, it explains why smaller apertures have a smaller upper bound in the size of particles that can be trapped. It is clear that further research has to be done concerning this topic. However, to do this a proper model for imaged CS after the lens it is necessary. This model is in progress, but it is out of the scope of this work.

4. Conclusions

The 3D structure of the CS proposed to be a new tool for OT was analyzed. Their main features were highlighted and a method to characterize the capability of these fields to trap Rayleigh particles was presented. It was found that for the 900 μm aperture diameter, the maximum particle that could be trapped is 50 nm, whereas for the 465 μm one, the limit is lesser than 40 nm, which expresses a dependence between aperture diameter and particle size to be trapped. Although this method indicates what particles might be trapped in this regime, it does not exclude the possibility for trapping larger particles. Note that the plot-method can also be applied to any arbitrary field, not only CS. Moreover, it should also be stressed that this method does not require sophisticated cameras, owing that only the derivative of intensity per unit intensity is need. Finally, this work proposes the natural evolution of prove for speckle-field trapping techniques. Note that, by properly engineering pupils mask, different CS with particular statistical properties can be obtained. Then, as is mentioned in the [Introduction](#), CS could enable studies on optical binding, coherent matter wave transport or photophoretic forces with engineered statistical properties.

Acknowledgments

We are specially thankful with Dr. Carlos Saavedra and Dr. Néstor Bolognini for their valuable commentaries and discussions along the whole process of this work, and for revising this manuscript. This work was supported by Grants Milenio ICM P06-067F and PFB08024. A. Lencina acknowledges support from the FONCYT-Argentina through PICT 1343 and from the CONICYT-Chile through PBCT red 21. Juan Pablo Staforelli and Esteban Vera are supported by a CONICYT Phd scholarship.

References

- [1] A. Ashkin, P. Natl. Acad. Sci. USA 94 (1997) 4853.
- [2] J.R. Moffitt, Y.R. Chemla, S.B. Smith, C. Bustamante, Annu. Rev. Biochem. 77 (2008) 205.
- [3] U. Mirsaidov, W. Timp, K. Timp, M. Mir, P. Matsudaira, G. Timp, Phys. Rev. E 78 (2008) 0219101.
- [4] G. Gibson, et al., Opt. Express 16 (2008) 14561.
- [5] B. Sun, Y. Roichman, D.G. Grier, Opt. Express 16 (2008) 15765.
- [6] D.G. Grier, Y. Roichman, Appl. Opt. 45 (2006) 880.
- [7] D.G. Grier, Nature 424 (2003) 810.
- [8] D. Boiron, C. Mennerat-Robilliard, J.M. Fournier, L. Guidoni, C. Salomon, G. Grynberg, Eur. Phys. J. D 7 (1999) 373.
- [9] G. Grynberg, P. Horak, C. Mennerat-Robilliard, Europhys. Lett. 49 (2000) 424.
- [10] R.C. Kuhn, O. Sigwarth, C. Miniatura, D. Delande, C.A. Müller, New J. Phys. 9 (2007) 1.
- [11] M. Lewenstein, A. Sanpera, V. Ahufinger, B. Damski, A. Sen, U. Sen, Adv. Phys. 56 (2007) 243.
- [12] Vladlen G. Shvedov, Andrei V. Rode, Yana V. Izdebskaya, Anton S. Desyatnikov, Wieslaw Krolikowski, Yuri S. Kivshar, Opt. Express 18 (2010) 3137.
- [13] P. Kner, B.B. Chhun, E.R. Griffiths, L. Winoto, M.G.L. Gustafsson, Nat. Methods 6 (2009) 339.
- [14] K. Uno, J. Uozumi, T. Asakura, Opt. Commun. 114 (1995) 203.
- [15] A. Lencina, M. Tebaldi, P. Vaveliuk, N. Bolognini, Wave. Random Complex Media 17 (2007) 29.
- [16] F. Mosso, M. Tebaldi, A. Lencina, N. Bolognini, Opt. Commun. 283 (2010) 1285.
- [17] M. Guizar-Sicairos, S.T. Thurman, J.R. Fienup, Opt. Lett. 33 (2008) 156.
- [18] K. Neuman, S. Block, Rev. Sci. Instrum. 75 (2004) 2787.